Antimatter ${}^{4}_{\Lambda}$H hypernucleus production and the ${}^{3}_{\Lambda}$H/^{3}He puzzle in relativistic heavy-ion collisions

Kai-Jia Sun[1] and Lie-Wen Chen[1,2,*]

[1]*Department of Physics and Astronomy and Shanghai Key Laboratory for Particle Physics and Cosmology, Shanghai Jiao Tong University, Shanghai 200240, China*

[2]*Center of Theoretical Nuclear Physics, National Laboratory of Heavy Ion Accelerator, Lanzhou 730000, China*

(Received 26 April 2016; published 29 June 2016)

We show that the measured yield ratio ${}^{3}_{\Lambda}$H/^{3}He (${}^{3}_{\Lambda}\overline{\mathrm{H}}$/${}^{3}\overline{\mathrm{He}}$) in Au + Au collisions at $\sqrt{s_{NN}} = 200$ GeV and in Pb + Pb collisions at $\sqrt{s_{NN}} = 2.76$ TeV can be understood within a covariant coalescence model if (anti-)Λ particles freeze out earlier than (anti-)nucleons but their relative freeze-out time is closer at $\sqrt{s_{NN}} = 2.76$ TeV than at $\sqrt{s_{NN}} = 200$ GeV. The earlier (anti-)Λ freeze-out can significantly enhance the yield of (anti)hypernucleus ${}^{4}_{\Lambda}$H (${}^{4}_{\Lambda}\overline{\mathrm{H}}$), leading to that ${}^{4}_{\Lambda}\overline{\mathrm{H}}$ has a comparable abundance with ${}^{4}\overline{\mathrm{He}}$ and thus provides an easily measured antimatter candidate heavier than ${}^{4}\overline{\mathrm{He}}$. The future measurement on ${}^{4}_{\Lambda}$H (${}^{4}_{\Lambda}\overline{\mathrm{H}}$) would be very useful to understand the (anti-)Λ freeze-out dynamics and the production mechanism of (anti)hypernuclei in relativistic heavy-ion collisions.

DOI: 10.1103/PhysRevC.93.064909

I. INTRODUCTION

The recent observations of light antinuclei in relativistic heavy-ion collisions at the Relativistic Heavy-Ion Collider (RHIC) [1,2] and Large Hadron Collider (LHC) [3,4] attract strong interest in the study of antimatter [5] and verify the general principles of quantum field theory, which requires that each particle has its corresponding antiparticle and any physical system has an antimatter analog with an identical mass (but the opposite charge). These studies also provide the possibility in laboratories to test the fundamental CPT theorem [6], to explore the interactions between antimatter and antimatter [7], and to help hunting for antimatter and dark matter in the universe through cosmic radiation observations [8]. The antihelium-4 (${}^{4}\overline{\mathrm{He}}$ or $\overline{\alpha}$) is the heaviest antimatter nucleus observed so far [2], and it is of great interest to search for antimatter nuclei heavier than ${}^{4}\overline{\mathrm{He}}$ in heavy-ion collisions, which is extremely useful for understanding the production mechanism of heavier antimatter [9,10].

Collisions of heavy nuclei at high energies also provide an abundant source of (anti)strangeness [11] and a unique tool to produce light (anti-)hypernuclei [12]. The STAR Collaboration at RHIC reported the observation of hypertriton (${}^{3}_{\Lambda}$H) and antihypertriton (${}^{3}_{\Lambda}\overline{\mathrm{H}}$) in Au + Au collisions at $\sqrt{s_{NN}} = 200$ GeV [13], and recently the ALICE Collaboration at LHC also reported the observation in Pb + Pb collisions at $\sqrt{s_{NN}} = 2.76$ TeV [14]. The value of measured yield ratio ${}^{3}_{\Lambda}$H/^{3}He is $0.82 \pm 0.16(\mathrm{stat.}) \pm 0.12(\mathrm{syst.})$ for 0%–80% centrality Au + Au collisions at $\sqrt{s_{NN}} = 200$ GeV (RHIC) [13] and $0.47 \pm 0.10(\mathrm{stat.}) \pm 0.13(\mathrm{syst.})$ in central (0%–10% centrality) Pb + Pb collisions at $\sqrt{s_{NN}} = 2.76$ TeV (LHC) [14]. It is thus favored that the measured ${}^{3}_{\Lambda}$H/^{3}He ratio at RHIC is higher than that at LHC, although they are compatible with a very small overlap within the uncertainties by combing the statistical and systematic uncertainties, i.e., 0.82 ± 0.20 at RHIC and 0.47 ± 0.16 at LHC. The value of the ${}^{3}_{\Lambda}$H/^{3}He ratio for 0%–80% centrality at RHIC (i.e., 0.82 ± 0.20) is expected to be further enhanced for central collisions because the ALICE measurements indicate that the ${}^{3}_{\Lambda}$H/^{3}He ratio in central Pb + Pb collisions is higher than that in peripheral Pb + Pb collisions [14]. A similar conclusion is obtained for the ${}^{3}_{\Lambda}\overline{\mathrm{H}}$/${}^{3}\overline{\mathrm{He}}$ ratio for which the measured value is $0.89 \pm 0.28(\mathrm{stat.}) \pm 0.13(\mathrm{syst.})$ for 0%–80% centrality Au + Au collisions at $\sqrt{s_{NN}} = 200$ GeV [13] and $0.42 \pm 0.10(\mathrm{stat.}) \pm 0.13(\mathrm{syst.})$ in central (0%–10% centrality) Pb + Pb collisions at $\sqrt{s_{NN}} = 2.76$ TeV [14]. As shown in Ref. [14], the conventional (statistical) thermal models [15–18] failed to describe the RHIC ratio, although some of them [15–17] successfully described the LHC ratio. The thermal model with a multi-freeze-out configuration [19] reasonably described the ratio at RHIC but failed at LHC, and so did the parton and hadron cascade plus dynamically constrained phase-space coalescence model [20,21]. The dynamical [22] and simple [23,24] coalescence models described marginally the ratio at RHIC but no results are available at LHC. Therefore, the measured ${}^{3}_{\Lambda}$H/^{3}He and ${}^{3}_{\Lambda}\overline{\mathrm{H}}$/${}^{3}\overline{\mathrm{He}}$ ratios challenge all theoretical calculations performed so far and call for novel mechanisms for (anti-)hypernuclei production in these collisions.

Because hyperons have quite different interactions compared with nucleons [25], they are expected to have different freeze-out dynamics in heavy-ion collisions, which will lead to distinct features for the production of light (anti)hypernuclei compared with that of light normal (anti)nuclei. In this work, we show that the covariant coalescence model can naturally reproduce the measured ${}^{3}_{\Lambda}$H/^{3}He (${}^{3}_{\Lambda}\overline{\mathrm{H}}$/${}^{3}\overline{\mathrm{He}}$) at both RHIC and LHC if (anti-)Λ particles freeze out earlier than (anti)nucleons but their relative freeze-out time is closer at LHC than at RHIC. The earlier anti-Λ ($\overline{\Lambda}$) freeze out leads to that the heavier antihypernucleus ${}^{4}_{\Lambda}\overline{\mathrm{H}}$ has a yield comparable to that of ${}^{4}\overline{\mathrm{He}}$ and thus provides an easily measured candidate for antimatter heavier than ${}^{4}\overline{\mathrm{He}}$.

II. COVARIANT COALESCENCE MODEL

We use the covariant coalescence model [26] for the production of light clusters in heavy-ion collisions. The

*Corresponding author: lwchen@sjtu.edu.cn

main feature of the coalescence model [27–29] is that the coalescence probability depends on the details of the phase-space structure of the constituent particles at freeze-out as well as the statistical weight and internal structure (wave function) of the coalesced cluster, and these details are of no relevance in the thermal model [15,16,30–32] of cluster creation.

The phase-space configuration of the constituent particles at freeze-out is a basic ingredient in the coalescence model, and, in principle, it can be obtained dynamically from transport model simulations for heavy-ion collisions (see, e.g., Refs. [33–37]). For the particle production at midrapidity in central heavy-ion collisions at RHIC and LHC considered here, for simplicity, we assume a boost-invariant longitudinal expansion for the constituent particles which are emitted from a freeze-out hypersurface Σ^μ, and the Lorentz invariant one-particle momentum distribution is then given by

$$E\frac{d^3N}{d^3p} = \frac{d^3N}{p_T dp_T d\phi_p dy} = \int_{\Sigma^\mu} d\sigma_\mu p^\mu f(x,p) = \int d^4x S(x,p), \quad (1)$$

where σ_μ denotes the normal vector of hypersurface Σ^μ and p^μ is the four-momentum of the emitted particle. The emission function $S(x,p)$ can be expressed by

$$S(x,p)d^4x = m_T \cosh(\eta - y) f(x,p) J(\tau)\tau d\tau d\eta r dr d\phi_s, \quad (2)$$

where we use longitudinal proper time $\tau = \sqrt{t^2 - z^2}$, spacetime rapidity $\eta = \frac{1}{2}\ln\frac{t-z}{t+z}$, cylindrical coordinates $(r,\ \phi_s)$, rapidity $y = \frac{1}{2}\ln(\frac{E+p_z}{E-p_z})$, transverse momentum (p_T,ϕ_p), and transverse mass $m_T = \sqrt{m^2 + p_T^2}$. The statistical distribution function $f(x,p)$ is given by $f(x,p) = g(2\pi)^{-3}[\exp(p^\mu u_\mu/kT)/\xi \pm 1]^{-1}$, with g being the spin degeneracy factor, ξ the fugacity, u_μ the four-velocity of a fluid element in the fireball, T the local temperature, and $p^\mu u_\mu = m_T \cosh\rho \cosh(\eta - y) - p_T \sinh\rho \cos(\phi_p - \phi_s)$ the energy in the local rest frame of the fluid. Following Ref. [38], we assume the freeze-out time follows a Gaussian distribution $J(\tau) = \frac{1}{\Delta\tau\sqrt{2\pi}}\exp[-\frac{(\tau-\tau_0)^2}{2(\Delta\tau)^2}]$ with a mean value τ_0 and a dispersion $\Delta\tau$ and the transverse rapidity distribution of the fluid element in the fireball is parameterized as $\rho = \rho_0 r/R_0$, with ρ_0 being the maximum transverse rapidity and R_0 the transverse radius of the fireball. The phase-space freeze-out configuration of the constituent particles is thus determined by six parameters, i.e., T, ρ_0, R_0, τ_0, $\Delta\tau$, and ξ.

The cluster production probability is determined by the overlap of the cluster Wigner function with the constituent particle phase-space distribution at freeze-out. If M particles are coalesced into a cluster, the invariant momentum distribution of the cluster can be obtained as

$$E\frac{d^3N_c}{d^3P} = Eg_c \int \left[\prod_{i=1}^{M}\frac{d^3p_i}{E_i}d^4x_i S(x_i,p_i)\right] \times \rho_c^{\mathrm{W}}(x_1,\ldots,x_M;\ p_1,\ldots,p_M)\delta^3\left(\mathbf{P} - \sum_{i=1}^{M}\mathbf{p_i}\right), \quad (3)$$

where N_c is the cluster multiplicity, E ($\mathbf{P}$) is its energy (momentum), g_c is the coalescence factor, and ρ_c^{W} is the Wigner function. In this work, the harmonic oscillator wave functions are assumed for all the clusters in the rest frame except the (anti)deuterons, for which the Hulthén wave function is used (see, e.g., Refs. [33,34]), and so the cluster Wigner functions and root-mean-square radii r_{rms} can be obtained analytically. The details about how to calculate the integral (3) can be found in Ref. [10]. It should be stressed that because the constituent particles may have different freeze-out time, the particles that freeze out earlier are allowed to propagate freely until the time when the last particles in the cluster freezes out to make the coalescence at equal time [10,33,35].

III. PRODUCTION OF (ANTI)HYPERTRITON

The coalescence factor is given by $g_c = \frac{2j+1}{2^N}$ [28] with j the spin and N the nucleon number of the nucleus. For d, ^{3}He, $^3_\Lambda$H, ^{4}He, and $^4_\Lambda$H that we focus on here, their spins are 1, 1/2, 1/2, 0 and 0, respectively, and their r_{rms}, which are directly related to their Wigner functions [10], are 1.96, 1.76, 4.9, 1.45, and 2.0 fm, respectively [39,40]. The anti(hyper)nuclei are assumed to have the same j and r_{rms} as their corresponding (hyper)nuclei.

Following Ref. [10], the proton (p) freeze-out parameters T and ρ_0 can be extracted from fitting the p spectrum, and the R_0, τ_0, $\Delta\tau$, and ξ_p can be obtained by further fitting the spectra of d and ^{3}He in the coalescence model. For central Au + Au collisions at $\sqrt{s_{NN}} = 200$ GeV, we obtain $T = 111.6$ MeV, $\rho_0 = 0.98$, $R_0 = 15.6$ fm, $\tau_0 = 10.6$ fm/c, $\Delta\tau = 3.5$ fm/c, and $\xi_p = 10.5$ by fitting the p spectrum from PHENIX [41] and the spectra of d and ^{3}He from STAR [1], and for antiprotons ($\overline{p}$), we assume they have the same freeze-out as protons except the fugacity is reduced to $\xi_{\overline{p}} = 7.84$ to describe the measured $\overline{p}/p = 0.75$ [41]. For central Pb + Pb collisions at $\sqrt{s_{NN}} = 2.76$ TeV, we obtain $T = 121.1$ MeV, $\rho_0 = 1.215$, $R_0 = 19.7$ fm, $\tau_0 = 15.5$ fm/c, $\Delta\tau = 1.0$ fm/c, and $\xi_p = 3.72$ by fitting the measured spectra of p, d, and ^{3}He from ALICE [1,4,42], and the antiprotons are assumed to have the same freeze-out parameters as protons because the $\overline{p}/p$ is close to unity at LHC. For neutrons (n) [antineutrons ($\overline{n}$), we take their freeze-out parameters as those of p's ($\overline{p}$'s) because the isospin chemical potential at freeze-out is small at RHIC and LHC [15]. The p freeze-out parameters at RHIC (denoted by FOAu-N) and LHC (denoted by FOPb-N) are summarized in Table I, and the freeze-out hypersurface at LHC is seen to have larger T, ρ_0, R_0, and τ_0 but smaller $\Delta\tau$ and ξ_p. In Fig. 1, the experimental data are compared with the calculated results for the spectra of p, d, and ^{3}He with FOAu-N and FOPb-N, and one can see that the coalescence model describes well the measured spectra. Table II lists the p_T-integrated yield in the midrapidity region ($-0.5 \leqslant y \leqslant 0.5$) (i.e., dN/dy) for p ($\overline{p}$), d ($\overline{d}$), ^{3}He ($^3\overline{\mathrm{He}}$), and ^{4}He ($^4\overline{\mathrm{He}}$) with FOAu-N and FOPb-N, and it is seen that the dN/dy values of d, ^{3}He, and ^{4}He ($\overline{d}$, $^3\overline{\mathrm{He}}$, and $^4\overline{\mathrm{He}}$) at LHC are roughly two (four) times as large as those at RHIC.

For Λ particles, we first assume they have the same freeze-out configuration as nucleons except that the Λ fugacity becomes $\xi_\Lambda = 42.8(9.54)$ at RHIC (LHC) by fitting the

TABLE I. Parameters of various freeze-out configurations for (anti)nucleons and (anti-)Λ particles at midrapidity in central collisions of Au + Au at $\sqrt{s_{NN}} = 200$ GeV (FOAu) and Pb + Pb at $\sqrt{s_{NN}} = 2.76$ TeV (FOPb). The unit of τ_0 and $\Delta\tau$ is fm/c. ξ and $\bar{\xi}$ denote the fugacity of particles and antiparticles, respectively.

	T (MeV)	ρ_0	R_0 (fm)	τ_0	$\Delta\tau$	ξ	$\bar{\xi}$
FOAu-N	111.6	0.980	15.6	10.6	3.5	10.5	7.84
FOPb-N	121.1	1.215	19.7	15.5	1.0	3.72	3.72
FOAu-Λ	111.6	0.980	15.6	10.6	3.5	42.8	35.1
FOPb-Λ	121.1	1.215	19.7	15.5	1.0	9.54	9.54
FOAu-Λ*	126.0	0.890	11.1	7.54	3.5	35.1	28.8
FOPb-Λ*	123.4	1.171	16.7	13.1	1.0	13.6	13.6

experimental Λ spectra [43,44], as shown in Fig. 2 by solid lines. The $\overline{\Lambda}$ particles are assumed to have the same freeze-out parameters as Λ particles, except the fugacity at RHIC is reduced to $\xi_{\overline{\Lambda}} = 35.1$ to describe the measured $\overline{\Lambda}/\Lambda = 0.82$ [43]. The (anti-)Λ freeze-out parameters are listed as FOAu-Λ (FOPb-Λ) in Table I for the central Au + Au (Pb + Pb) collisions. With FOAu-Λ and FOPb-Λ (together with FOAu-N and FOPb-N), the spectra of $^3_\Lambda$H and $^4_\Lambda$H can then be calculated using the coalescence model, and the results are shown in Fig. 1. The dN/dy values for Λ ($\overline{\Lambda}$), $^3_\Lambda$H ($^3_{\overline{\Lambda}}\overline{\text{H}}$), and $^4_\Lambda$H ($^4_{\overline{\Lambda}}\overline{\text{H}}$) are summarized in Table II, and the resulting $^3_\Lambda$H/^{3}He is about 0.29 (0.24) at RHIC (LHC) with FOAu-Λ (FOPb-Λ), which significantly underestimates the measured values from STAR [13] and ALICE [14], i.e., $0.82 \pm 0.16(\text{stat.}) \pm 0.12(\text{syst.})$ for 0%–80% centrality Au + Au collisions at $\sqrt{s_{NN}} = 200$ GeV [13] and $0.47 \pm 0.10(\text{stat.}) \pm 0.13(\text{syst.})$ in central (0%–10% centrality) Pb + Pb collisions at $\sqrt{s_{NN}} = 2.76$ TeV [14]. The predicted ratio $^3_{\overline{\Lambda}}\overline{\text{H}}/^3\overline{\text{He}}$ is about 0.31 (0.24) at RHIC (LHC)

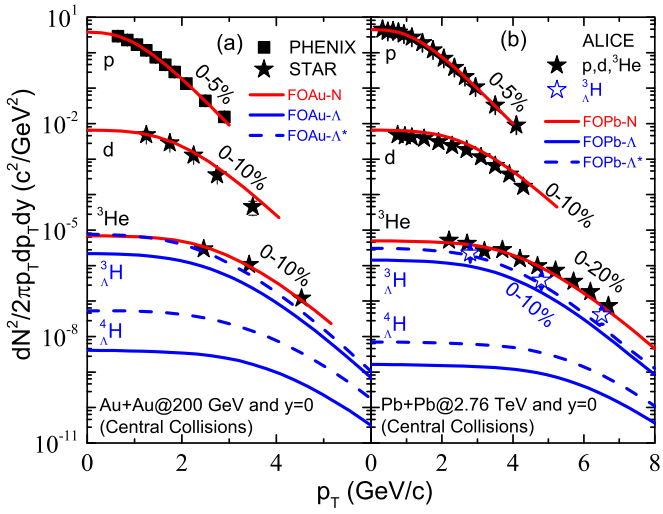

FIG. 1. Transverse momentum distributions of p, d, ^{3}He, $^3_\Lambda$H, and $^4_\Lambda$H at midrapidity in central collisions of Au + Au at $\sqrt{s_{NN}} =$ 200 GeV (a) and Pb + Pb at $\sqrt{s_{NN}} = 2.76$ TeV (b) predicted by a coalescence model with various freeze-out configurations. For Au + Au collisions, the data of protons are taken from the PHENIX [41] and those of d and ^{3}He are taken from STAR [1]. The data of p, d, ^{3}He, and $^3_\Lambda$H for Pb + Pb collisions are taken from ALICE [4,14,42].

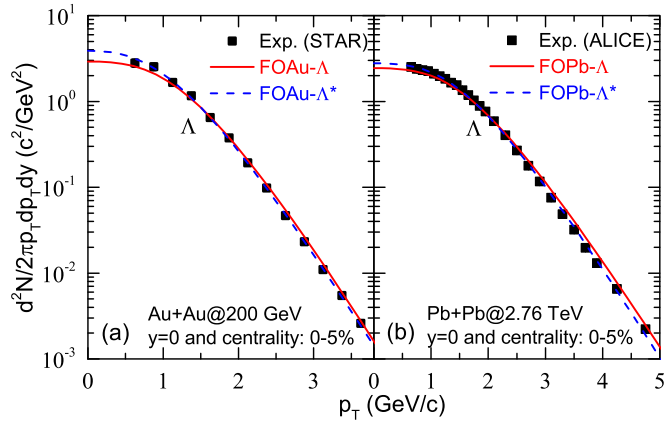

FIG. 2. Transverse momentum distribution of Λ's in central collisions of Au + Au at $\sqrt{s_{NN}} = 200$ GeV (a) and Pb + Pb at $\sqrt{s_{NN}} = 2.76$ TeV (b) from coalescence model calculations with various freeze-out configurations. The experimental data are taken from STAR [43] for the Au + Au collisions and from ALICE [44] for the Pb + Pb collisions.

with FOAu-Λ (FOPb-Λ), again significantly underestimating the measured values, i.e., $0.89 \pm 0.28(\text{stat.}) \pm 0.13(\text{syst.})$ from STAR [13] and $0.42 \pm 0.10(\text{stat.}) \pm 0.13(\text{syst.})$ from ALICE [14]. In addition, the predicted $^3_\Lambda$H spectrum with FOPb-Λ is seen to underestimate the recently measured spectrum by ALICE [14].

To understand the disagreement of $^3_\Lambda$H/^{3}He ($^3_{\overline{\Lambda}}\overline{\text{H}}/^3\overline{\text{He}}$) and the $^3_\Lambda$H spectrum between the predictions and the measurements, we extract the Λ freeze-out parameters T and ρ_0 by directly fitting the measured Λ spectra [43,44] as shown in Fig. 2 by dashed lines, and we obtain $T = 126(123.4)$ MeV and $\rho_0 = 0.89(1.171)$ for Au + Au (Pb + Pb) collisions, which better describe the data than FOAu-Λ (FOPb-Λ). The Λ particles thus have a higher freeze-out temperature than nucleons, especially at RHIC, implying an earlier freeze-out for Λ particles than for nucleons, which is consistent with the empirical picture that the strange baryons usually freeze-out earlier than the nonstrange baryons owing to their relatively smaller interaction cross sections. The earlier Λ freeze-out is also supported by the investigation on strangeness production [19,45–48], as well as the microscopic transport model simulations [49].

An earlier Λ freeze-out means the Λ particles can pick up un-frozen-out nucleons to form light hypernuclei, and this implies that the nucleons coalesced into light hypernuclei also have an earlier freeze-out time than those coalesced into normal light nuclei. To consider this effect, for the coalescence production of light hypernuclei, we reduce the τ_0 and R_0 simultaneously but increase the ξ to fit the Λ and p spectra. In this way, the earlier freeze-out increases the phase-space density of Λ, p, and n, and thus the $^3_\Lambda$H production rate. To fit the measured central value 0.82 (0.47) of the $^3_\Lambda$H/^{3}He ratio at RHIC (LHC), we find the R_0 and τ_0 need to be reduced to 71% (85%) of their values in FOAu-Λ (FOPb-Λ), i.e., $R_0 = 11.1(16.7)$ fm and $\tau_0 = 7.54(13.1)$ fm/c, if we fix

TABLE II. dN/dy at midrapidity of light (anti)(hyper)hypernuclei for various freeze-out configurations in central collisions of Au + Au at $\sqrt{s_{NN}} = 200$ GeV (FOAu) and Pb + Pb at $\sqrt{s_{NN}} = 2.76$ TeV (FOPb).

	$p(\overline{p})$	$d(\overline{d})$	^{3}He($^3\overline{\text{He}}$)	^{4}He($^4\overline{\text{He}}$)
FOAu-N	16.1(12.1)	$7.49(4.21) \times 10^{-2}$	$14.9(6.29) \times 10^{-5}$	$15.4(4.88) \times 10^{-8}$
FOPb-N	33.5(33.5)	$15.0(15.0) \times 10^{-2}$	$2.36(2.36) \times 10^{-4}$	$2.20(2.20) \times 10^{-7}$
	$\Lambda(\overline{\Lambda})$		${}^3_\Lambda\text{H}({}^3_{\overline{\Lambda}}\overline{\text{H}})$	${}^4_\Lambda\text{H}({}^4_{\overline{\Lambda}}\overline{\text{H}})$
FOAu-Λ	17.0(14.0)		$4.26(1.96) \times 10^{-5}$	$14.8(5.12) \times 10^{-8}$
FOPb-Λ	24.9(24.9)		$5.72(5.72) \times 10^{-5}$	$1.36(1.36) \times 10^{-7}$
FOAu-Λ^*	18.8(15.4)		$12.3(5.65) \times 10^{-5}$	$15.7(5.43) \times 10^{-7}$
FOPb-Λ^*	25.9(25.9)		$1.12(1.12) \times 10^{-4}$	$5.43(5.43) \times 10^{-7}$

$T = 126(123.4)$ MeV, $\rho_0 = 0.89(1.171)$, and $\Delta\tau = 3.5(1.0)$ fm/c. These new freeze-out configurations are denoted as FOAu-Λ^* and FOPb-Λ^* in Table I. It is interesting to note that the Λ freeze-out temperature is slightly higher at RHIC than at LHC. For FOAu-Λ^* and FOPb-Λ^*, we have neglected final-state interactions of the produced ${}^3_\Lambda$H during the last 2–3 fm/c time interval when some nucleons have not yet frozen out, and probably this can be justified from the transport model study which indicates including the final-state interactions changes the deuteron yield by only about 20% at RHIC [36]. However, because ${}^3_\Lambda$H is an even more loosely bound system than deuteron (note that the total binding energy of ${}^3_\Lambda$H is 2.354 MeV with the Λ separation energy of only about 0.13 MeV [50], and the total binding energy of deuteron is 2.224 MeV [51]), the effects of the final-state interactions on ${}^3_\Lambda$H yield are thus expected to be stronger than that on deuteron. For ${}^4_\Lambda$H, the total binding energy is 10.601 MeV with the Λ separation energy of 2.12 MeV [52], and the effects of the final-state interactions are thus expected to be similar with the case of deuteron. The quantitative information on the final interaction effects needs complicated transport model simulations. The stronger final-state interaction (destruction) of ${}^3_\Lambda$H implies that the Λ particles need an even earlier freeze-out than that obtained above, and the effects of an earlier Λ freeze-out in the present work are thus considered to be conservative estimate.

The predicted spectra of ${}^3_\Lambda$H and ${}^4_\Lambda$H with FOAu-Λ^* and FOPb-Λ^* are shown in Fig. 1 by dashed lines, and one can see that compared with FOAu-Λ and FOPb-Λ, FOAu-Λ^*, and FOPb-Λ^* significantly enhance the production of ${}^3_\Lambda$H and ${}^4_\Lambda$H and now the ${}^3_\Lambda$H spectra measured by ALICE [14] can be reasonably described by FOPb-Λ^*. The dN/dy values for Λ ($\overline{\Lambda}$), ${}^3_\Lambda$H (${}^3_{\overline{\Lambda}}\overline{\text{H}}$), and ${}^4_\Lambda$H (${}^4_{\overline{\Lambda}}\overline{\text{H}}$) with FOAu-$\Lambda^*$ and FOPb-Λ^* are listed in Table II. The small difference for the dN/dy of (anti-)Λ between FOAu-Λ^* (FOPb-Λ^*) and FOAu-Λ (FOPb-Λ) is attributable to the slight variation of the Λ spectra from different fits, as shown in Fig. 2. The calculated ${}^3_\Lambda\text{H}/{}^3\text{He}$ and ${}^3_{\overline{\Lambda}}\overline{\text{H}}/{}^3\overline{\text{He}}$ ratios are, respectively, about 0.83 (0.47) and 0.91 (0.47) at RHIC (LHC) with FOAu-Λ^* (FOPb-Λ^*), nicely reproducing the measured central values. Therefore, our results suggest that the (anti-)Λ particles may freeze out earlier than (anti)nucleons but their relative freeze-out time is closer at LHC than at RHIC. It is interesting to see that the Λ and nucleon freeze-out parameters seem to come close to each other as the energy increases and this is understandable because a higher colliding energy generally leads to a longer-lived hadronic fireball, where the Λ's and nucleons will experience more collisions.

The ratio $S_3 = {}^3_\Lambda\text{H}/({}^3\text{He} \times \Lambda/p)$ was first suggested in Ref. [53] in the expectation that dividing the strange to nonstrange baryon yield should result in a value near unity in a naive coalescence model. It was also argued [22] to be a good representation of the local correlation between baryon number and strangeness [54], and thus should be a valuable probe for the onset of deconfinement in relativistic heavy-ion collisions. The S_3 was measured to be 1.08 ± 0.22 for 0%–80% centrality Au + Au collisions [13] and $0.60 \pm 0.13(\text{stat.}) \pm 0.21(\text{syst.})$ for central (0-10% centrality) Pb + Pb collisions [14]. For central collisions considered here, the S_3 for Au + Au (Pb + Pb) collisions is 0.27 (0.33) with FOAu-Λ (FOPb-Λ), while it increases to 0.71 (0.61) with FOAu-Λ^* (FOPb-Λ^*). The FOAu-Λ (FOPb-Λ) thus significantly underestimates the measured S_3 for Au + Au (Pb + Pb) collisions. While FOPb-Λ^* nicely reproduces the measured S_3 for Pb + Pb collisions, the FOAu-Λ^* still underestimates the measured S_3 for Au + Au collisions. It should be noted that while there is negligible feed-down from heavier states into ${}^3_\Lambda$H and ^{3}He, the Λ and p are significantly influenced by feed-down from decays of excited baryonic states. In the coalescence model calculations, the Λ and p from the short-lived strong decays are included because they appear in the fireball, while those from the other long-lived decays are excluded because they are out of the fireball. In the calculation of the S_3 for Au + Au collisions, we use the p spectrum from PHENIX [41], which is corrected by excluding the contribution from the long-lived weak decays. We note that including 40% contribution from weak decays to the p yield leads to $S_3 = 0.994$ for Au + Au collisions with FOPb-Λ^*, consistent with the measured value from STAR.

It should be pointed out that although the Λ's and nucleons are assumed to have the same freeze-out configuration, the S_3 is still significantly less than unity [e.g., $S_3 = 0.27$ (0.32) for FOAu-Λ (FOPb-Λ)]. This is mainly attributable to the much larger size of ${}^3_\Lambda$H than that of ^{3}He, as suggested first in Ref. [53]. To see this more clearly, we show in Fig. 3 the predicted dN/dy of ${}^3_\Lambda$H and ^{3}He as a function of their root-mean-square radii in central collisions of Au + Au at $\sqrt{s_{NN}} = 200$ GeV and Pb + Pb at $\sqrt{s_{NN}} = 2.76$ TeV from the coalescence model with various freeze-out configurations. The empirical size values, i.e., $r_{\text{rms}} = 4.9$ fm for ${}^3_\Lambda$H and $r_{\text{rms}} = 1.76$ fm for ^{3}He are also indicated in Fig. 3. It is seen that, because of the finite-size

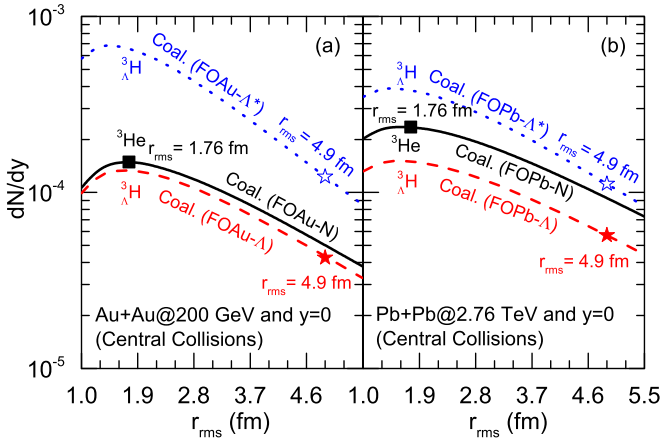

FIG. 3. The predicted dN/dy of $^3_\Lambda$H and ^{3}He at midrapidity as a function of their root-mean-square radii $r_{\rm rms}$ in central collisions of Au + Au at $\sqrt{s_{NN}} = 200$ GeV (a) and Pb + Pb at $\sqrt{s_{NN}} = 2.76$ TeV (b) from the coalescence model with various freeze-out configurations. The stars (squares) indicate the empirical size values $r_{\rm rms} = 4.9(1.76)$ fm for $^3_\Lambda$H (^{3}He).

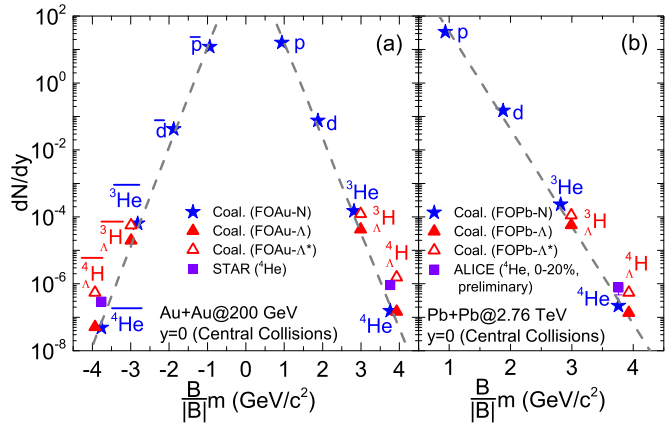

FIG. 4. The predicted dN/dy of light (anti)(hyper)nuclei at midrapidity as a function of $\frac{B}{|B|}m$ in central collisions of Au + Au at $\sqrt{s_{NN}} = 200$ GeV (a) and Pb + Pb at $\sqrt{s_{NN}} = 2.76$ TeV (b) from the coalescence model with various freeze-out configurations. The squares in (a) represent the results for ^{4}He and $^4\overline{\rm He}$ in the Au + Au collisions by considering the binding energy effects to fit STAR data [2,10] while the square in (b) is the preliminary result for ^{4}He in 0%–20% centrality Pb + Pb collisions from ALICE measurement [58].

cutoff effect of the fireball in the spatial part integration of Eq. (3), the dN/dy decrease with $r_{\rm rms}$ when $r_{\rm rms}$ is larger than about 1.6 fm. Furthermore, it is interesting to see that the dN/dy exhibits a stronger $r_{\rm rms}$ dependence at RHIC than that at LHC, and this is attributable mainly to the fact that the freeze-out volume ($\pi R_0^2 \tau_0$) is smaller at RHIC. Compared with the thermal model, the coalescence model thus has a distinct feature that the cluster yield depends on the cluster size, as mentioned earlier. Assuming $^3_\Lambda$H has a same $r_{\rm rms}$ as ^{3}He, i.e., $r_{\rm rms} = 1.76$ fm, we find that the S_3 values for both Au + Au (with FOAu-Λ) and Pb + Pb (with FOPb-Λ) collisions are drastically enhanced to about 0.85 and further to unity if the Λ's and nucleons are assumed to have equal mass, as expected from the naive coalescence model.

IV. PRODUCTION OF $^4_\Lambda$H ($^4_{\overline{\Lambda}}\overline{\rm H}$)

The $^4_\Lambda$H is a well-researched hypernucleus with lifetime of 192^{+20}_{-18} ps [55] and mass $M(^4_\Lambda{\rm H}) = 3922.484 \pm 0.01({\rm stat.}) \pm 0.09({\rm syst.})$ MeV [52] [note the mass of ^{4}He is $M(^4{\rm He}) = 3727.379$ MeV]. The $^4_\Lambda$H can be identified through the ^{4}He-π^- invariant mass spectrum from the decay $^4_\Lambda{\rm H} \to {}^4{\rm He} + \pi^-$ with branching ratio of about 50% [56,57].

Shown in Fig. 4 are the predicted dN/dy of light (anti)(hyper)nuclei as a function of $\frac{B}{|B|}m$, where B is the baryon number of light clusters and m is the corresponding mass, in central collisions of Au + Au at $\sqrt{s_{NN}} = 200$ GeV and Pb + Pb at $\sqrt{s_{NN}} = 2.76$ TeV from the coalescence model with various freeze-out configurations. For the Pb + Pb collisions, we only show the results of (hyper)nuclei in Fig. 4 because the results of anti-(hyper)nuclei are the same as those of their corresponding (hyper)nuclei because the antiprotons (and anti-Λ's) are assumed to have the same freeze-out configuration as their corresponding particles in central Pb + Pb collisions at $\sqrt{s_{NN}} = 2.76$ TeV. Also included in Fig. 4 are the preliminary result for dN/dy (i.e., $7.8 \pm 3.1 \times 10^{-7}$) of ^{4}He in central (0%–20%) Pb + Pb collisions at $\sqrt{s_{NN}} = 2.76$ TeV recently measured by ALICE [58], as well as the results for dN/dy of ^{4}He and $^4\overline{\rm He}$ in central Au + Au collisions obtained from the coalescence model by considering the binding energy effects to fit the STAR data (for details, see Ref [10]). Because FOAu-N and FOPb-N describe well the spectra of p, d, and ^{3}He as shown in Fig. 1, the predicted dN/dy of p ($\overline{p}$), d ($\overline{d}$), and ^{3}He ($^3\overline{\rm He}$) in Fig. 4 are expected to give good estimates of the experimental data on dN/dy. However, FOAu-N and FOPb-N significantly underestimate the dN/dy of ^{4}He and $^4\overline{\rm He}$, and these discrepancies can be fixed by considering the effects of the large binding energy of ^{4}He and $^4\overline{\rm He}$ [10].

Furthermore, it is seen from Fig. 4 that, compared with FOAu-Λ (FOPb-Λ), FOAu-Λ* (FOPb-Λ*) significantly enhances the dN/dy of (anti-)$^3_\Lambda$H and (anti-)$^4_\Lambda$H owing to the earlier Λ freeze-out. From the detailed numbers listed in Table II, one can see that in Au + Au collisions, the dN/dy of $^4_\Lambda$H ($^4_{\overline{\Lambda}}\overline{\rm H}$) is 1.48×10^{-7} (5.12×10^{-8}) with FOAu-Λ and 1.57×10^{-6} (5.43×10^{-7}) with FOAu-Λ*, implying that the earlier Λ freeze-out enhances the yields of both $^4_\Lambda$H and $^4_{\overline{\Lambda}}\overline{\rm H}$ by a factor of 10.6. In Pb + Pb collisions, the dN/dy of $^4_\Lambda$H (same for $^4_{\overline{\Lambda}}\overline{\rm H}$) is 1.36×10^{-7} with FOPb-Λ and 5.43×10^{-7} with FOPb-Λ*, and the enhancement factor owing to the earlier Λ freeze-out is 4.0. It is interesting to see that the dN/dy of $^4_\Lambda$H ($^4_{\overline{\Lambda}}\overline{\rm H}$) at RHIC (with FOAu-Λ*) is about 3.5(1.0) times as large as that at LHC (with FOPb-Λ*), and the predicted yields of the heavier $^4_\Lambda$H ($^4_{\overline{\Lambda}}\overline{\rm H}$) at RHIC are larger than the measured ^{4}He ($^4\overline{\rm He}$) yield at RHIC (i.e., about 9.18×10^{-7} for ^{4}He and 2.91×10^{-7} for $^4\overline{\rm He}$ [10]). Also, the predicted dN/dy of $^4_\Lambda$H ($^4_{\overline{\Lambda}}\overline{\rm H}$) with FOPb-Λ* at LHC (i.e., 5.43×10^{-7}) is very close to the measured dN/dy of ^{4}He ($^4\overline{\rm He}$) (i.e., about $7.8 \pm 3.1 \times 10^{-7}$). The larger

yields of light (hyper)nuclei at lower colliding energies are also observed in the predictions of thermal models (see, e.g., Ref. [15]). Compared with ^{4}He ($^{\overline{4}}\overline{\mathrm{He}}$), the larger or comparable yields of $^4_\Lambda$H ($^{\overline{4}}_{\overline{\Lambda}}\overline{\mathrm{H}}$) are mainly attributable to the effects of earlier Λ freeze-out. Generally, the yields of anti-(hyper)nuclei increase with the colliding energy, and here that RHIC and LHC have the equal dN/dy of $^{\overline{4}}_{\overline{\Lambda}}\overline{\mathrm{H}}$ is mainly attributable to the stronger earlier-Λ-freeze-out effects at RHIC. The future experimental measurement on $^4_\Lambda$H ($^{\overline{4}}_{\overline{\Lambda}}\overline{\mathrm{H}}$) would be very useful to test the idea of earlier (anti-)Λ freeze-out.

V. CONCLUSION

The measured yield ratio $^3_\Lambda$H/^{3}He ($^{\overline{3}}_{\overline{\Lambda}}\overline{\mathrm{H}}/^{\overline{3}}\overline{\mathrm{He}}$) in heavy-ion collisions at RHIC and LHC can be naturally explained by the covariant coalescence model if the (anti-)Λ particles freeze out earlier than (anti-)nucleons but their relative freeze-out time is closer at LHC than at RHIC. The earlier (anti-)Λ freeze-out can significantly enhance the yield of $^4_\Lambda$H ($^{\overline{4}}_{\overline{\Lambda}}\overline{\mathrm{H}}$), leading to that $^{\overline{4}}_{\overline{\Lambda}}\overline{\mathrm{H}}$ provides an easily measured candidate for antimatter heavier than $^{\overline{4}}\overline{\mathrm{He}}$. The larger relative p-Λ (p-$\overline{\Lambda}$) freeze-out time difference at RHIC leads to a larger (equal) yield of $^4_\Lambda$H ($^{\overline{4}}_{\overline{\Lambda}}\overline{\mathrm{H}}$) at RHIC than at LHC. In the future, more precise measurement on $^3_\Lambda$H/^{3}He and $^{\overline{3}}_{\overline{\Lambda}}\overline{\mathrm{H}}/^{\overline{3}}\overline{\mathrm{He}}$ as well as the measurement on $^4_\Lambda$H and $^{\overline{4}}_{\overline{\Lambda}}\overline{\mathrm{H}}$ would be extremely helpful to test the proposed freeze-out scenario for (anti-)Λ particles and the predictions on light (anti-)hypernuclei production presented in this work.

ACKNOWLEDGMENTS

We are grateful to Vincenzo Greco, Che Ming Ko, Yu-Gang Ma, Zhang-Bu Xu, Zhong-Bao Yin, and Xian-Rong Zhou for helpful discussions. This work was supported in part by the Major State Basic Research Development Program (973 Program) in China under Contracts No. 2015CB856904 and No. 2013CB834405, the NSFC under Grants No. 11275125 and No. 11135011, the "Shu Guang" project supported by Shanghai Municipal Education Commission and Shanghai Education Development Foundation, the Program for Professor of Special Appointment (Eastern Scholar) at Shanghai Institutions of Higher Learning, and the Science and Technology Commission of Shanghai Municipality under Grant No. 11DZ2260700.

[1] B. I. Abelev *et al.* (STAR Collaboration), arXiv:0909.0566.
[2] (STAR Collaboration) H. Agakishiev *et al.*, Nature (London) **473**, 353 (2011).
[3] N. Sharma (for the ALICE Collaboration), J. Phys. G **38**, 124189 (2011).
[4] J. Adam *et al.* (ALICE Collaboration), Phys. Rev. C **93**, 024917 (2016).
[5] Y. G. Ma, J. H. Chen, and L. Xue, Front. Phys. **7**, 637 (2012); Y. G. Ma, J. Phys.: Conf. Ser. **420**, 012036 (2013); EPJ Web Conf. **66**, 04020 (2014).
[6] (ALICE Collaboration) J. Adam *et al.*, Nat. Phys. **11**, 811 (2015).
[7] (STAR Collaboration) L. Adamczyk *et al.*, Nature (London) **527**, 345 (2015).
[8] E. Carlson, A. Coogan, T. Linden, S. Profumo, A. Ibarra, and S. Wild, Phys. Rev. D **89**, 076005 (2014).
[9] W. Greiner, Int. J. Mod. Phys. E **05**, 1 (1996); J. Phys.: Conf. Ser. **413**, 012002 (2013).
[10] K. J. Sun and L. W. Chen, Phys. Lett. B **751**, 272 (2015).
[11] P. Koch, B. Müller, and J. Rafelski, Phys. Rep. **142**, 167 (1986).
[12] C. M. Ko, Phys. Rev. C **32**, 326 (1985).
[13] B. I. Abelev *et al.* (STAR Collaboration), Science **328**, 58 (2010).
[14] J. Adam *et al.* (ALICE Collaboration), Phys. Lett. B **754**, 360 (2016).
[15] A. Andronic, P. Braun-Munzinger, J. Stachel, and H. Stöcker, Phys. Lett. B **697**, 203 (2011).
[16] J. Cleymans, S. Kabana, I. Kraus, H. Oeschler, K. Redlich, and N. Sharma, Phys. Rev. C **84**, 054916 (2011).
[17] S. Pal and W. Greiner, Phys. Rev. C **87**, 054905 (2013).
[18] M. Petran, J. Letessier, V. Petracek, and J. Rafelski, Phys. Rev. C **88**, 034907 (2013).
[19] S. Chatterjee and B. Mohanty, Phys. Rev. C **90**, 034908 (2014).
[20] G. Chen, H. Chen, J. Wu, D. S. Li, and M. J. Wang, Phys. Rev. C **88**, 034908 (2013).
[21] Z. She, G. Chen, H. Xu, T. Zeng, and D. Li, arXiv:1509.06493.
[22] S. Zhang, J. H. Chen, H. Crawford, D. Keane, Y. G. Ma, and Z. B. Xu, Phys. Lett. B **684**, 224 (2010).
[23] L. Xue, Y. G. Ma, J. H. Chen, and S. Zhang, Phys. Rev. C **85**, 064912 (2012).
[24] N. Shah, Y. G. Ma, J. H. Chen, and S. Zhang, Phys. Lett. B **754**, 6 (2016).
[25] E. Botta, T. Bressani, and G. Garbarino, Eur. Phys. J. A **48**, 41 (2012).
[26] C. B. Dover, U. Heinz, and E. Schnedermann, Phys. Rev. C **44**, 1636 (1991).
[27] S. T. Butler and C. A. Pearson, Phys. Rev. Lett. **7**, 69 (1961).
[28] H. Sato and K. Yazaki, Phys. Lett. B **98**, 153 (1981).
[29] L. P. Csernai and J. I. Kapusta, Phys. Rep. **131**, 223 (1986).
[30] J. Cleymans, K. Redlich, and E. Suhonen, Z. Phys. C **51**, 137 (1991).
[31] P. Braun-Munzinger and J. Stachel, J. Phys. G **21**, L17 (1995); Nature (London) **448**, 302 (2007).
[32] J. Steinheimer, K. Gudima, A. Botvina, I. Mishustin, M. Bleicher, and H. Stöcker, Phys. Lett. B **714**, 85 (2012).
[33] R. Mattiello, H. Sorge, H. Stöcker, and W. Greiner, Phys. Rev. C **55**, 1443 (1997).
[34] L. W. Chen, C. M. Ko, and B. A. Li, Phys. Rev. C **68**, 017601 (2003); Nucl. Phys. A **729**, 809 (2003); Phys. Rev. C **69**, 054606 (2004).
[35] L. W. Chen and C. M. Ko, Phys. Rev. C **73**, 044903 (2006).
[36] Y. Oh, Z. W. Lin, and C. M. Ko, Phys. Rev. C **80**, 064902 (2009).
[37] L. Zhu, C. M. Ko, and X. Yin, Phys. Rev. C **92**, 064911 (2015).
[38] F. Retiére and M. A. Lisa, Phys. Rev. C **70**, 044907 (2004).
[39] G. Röpke, Phys. Rev. C **79**, 014002 (2009).
[40] H. Nemura, Y. Suzuki, Y. Fujiwara, and C. Nakamoto, Prog. Theor. Phys. **103**, 929 (2000).

[41] S. S. Adler *et al.* (PHENIX Collaboration), Phys. Rev. C **69**, 034909 (2004).
[42] B. Abelev *et al.* (ALICE Collaboration), Phys. Rev. Lett. **109**, 252301 (2012).
[43] G. Agakishiev *et al.* (STAR Collaboration), Phys. Rev. Lett. **108**, 072301 (2004).
[44] B. Abelev *et al.* (ALICE Collaboration), Phys. Rev. Lett. **111**, 222301 (2013).
[45] M. He, R. J. Fries, and R. Rapp, Phys. Rev. C **82**, 034907 (2010).
[46] K. A. Bugaev, D. R. Oliinychenko, J. Cleymans, A. I. Ivanytskyi, I. N. Mishustin, E. G. Nikonov, and V. V. Sagun, Europhys. Lett. **104**, 22002 (2013).
[47] S. Chatterjee, R. M. Godbole, and S. Gupta, Phys. Lett. B **727**, 554 (2013).
[48] S. Chatterjee, B. Mohanty, and R. Singh, Phys. Rev. C **92**, 024917 (2015).
[49] L. V. Bravina, K. Tywoniuk, and E. E. Zabrodin, J. Phys. G **31**, S989 (2005).
[50] M. Juric *et al.*, Nucl. Phys. B **52**, 1 (1973).
[51] M. Wang *et al.*, Chin. Phys. C **36**, 1603 (2012).
[52] A. Esser, S. Nagao, F. Schulz, P. Achenbach, C. Ayerbe Gayoso, R. Böhm, O. Borodina, D. Bosnar, V. Bozkurt, L. Debenjak, M. O. Distler, I. Friščić, Y. Fujii, T. Gogami, O. Hashimoto, S. Hirose, H. Kanda, M. Kaneta, E. Kim, Y. Kohl, J. Kusaka, A. Margaryan, H. Merkel, M. Mihovilovič, U. Müller, S. N. Nakamura, J. Pochodzalla, C. Rappold, J. Reinhold, T. R. Saito, A. Sanchez Lorente, S. Sánchez Majos, B. S. Schlimme, M. Schoth, C. Sfienti, S. Širca, Tang, M. Thiel, K. Tsukada, A. Weber, and K. Yoshida (A1 Collaboration), Phys. Rev. Lett. **114**, 232501 (2015).
[53] T. A. Armstrong, K. N. Barish, S. Batsouli, S. J. Bennett, M. Bertaina, A. Chikanian, S. D. Coe, T. M. Cormier, R. Davies, C. B. Dover, P. Fachini, B. Fadem, L. E. Finch, N. K. George, S. V. Greene, P. Haridas, J. C. Hill, A. S. Hirsch, R. Hoversten, H. Z. Huang, H. Jaradat, B. S. Kumar, T. Lainis, J. G. Lajoie, R. A. Lewis, Q. Li, B. Libby, R. D. Majka, T. E. Miller, M. G. Munhoz, J. L. Nagle, I. A. Pless, J. K. Pope, N. T. Porile, C. A. Pruneau, M. S. Z. Rabin, J. D. Reid, A. Rimai, A. Rose, F. S. Rotondo, J. Sandweiss, R. P. Scharenberg, A. J. Slaughter, G. A. Smith, X. M. L. Tincknell, W. S. Toothacker, G. Van Buren, F. K. Wohn, and Z. Xu (E864 Collaboration), Phys. Rev. C **70**, 024902 (2004).
[54] V. Koch, A. Majumder, and J. Randrup, Phys. Rev. Lett. **95**, 182301 (2005).
[55] C. Rappold *et al.*, Phys. Lett. B **728**, 543 (2014).
[56] I. Kumagai-Fuse, S. Okabe, and Y. Akaishi, Nucl. Phys. A **585**, 365 (1995).
[57] H. Outa, Nucl. Phys. A **639**, 251c (1998).
[58] N. Sharma (ALICE Collaboration), Nucl. Phys. A, arXiv:1602.02173.